

Effect of loading frequency and clay content on the dynamic properties of sandy-clay mixtures using cyclic triaxial tests

Alireza Hasibi Taheri^a, Navid Hadiani^{*}, S. Mohammad Ali Sadreddini^b and Mahmood Zakeri Nayeri^c

Islamic Azad University Islamshahr Branch, Tehran, Iran

(Received April 16, 2023, Revised October 18, 2023, Accepted November 16, 2023)

Abstract. Adopting a rational engineering methodology for building structures on sandy-clay soil layers has become increasingly important since it is crucial when structures erected on them often face seismic and cyclic wave loads. Such loads can cause a reduction in the stiffness, strength, and stability of the structure, particularly under un-drained conditions. Hence, this study aims to investigate how the dynamic properties of sand-clay mixtures are affected by loading frequency and clay content. Cyclic triaxial tests were performed on a total of 36 samples, comprising pure sand with a relative density of 60% and sand with varying percentages of clay. The tests were conducted under confining pressures of 50 and 100 kPa, and the samples' dynamic behavior was analyzed at loading frequencies of 0.1, 1, and 4 Hz. The findings indicate that an increase in confining pressure leads to greater inter-particle interaction and a reduced void ratio, which results in an increase in the soil's shear modulus. An increase in the shear strength and confinement of the samples led to a decrease in energy dissipation and damping ratio. Changes in loading frequency showed that as the frequency increased, the damping ratio decreased, and the strength of the samples increased. Increasing the loading frequency not only reflects changes in frequency but also reduces the relative permeability and enhances the resistance of samples. An analysis of the dynamic properties of sand and sand-clay mixtures indicates that the introduction of clay to a sand sample reduces the shear modulus and permeability properties.

Keywords: cyclic triaxial test; dynamic parameters; loading frequency; sandy-clay; shear modulus

1. Introduction

The dynamic properties of soil, including shear modulus (G) and damping ratio (D), play a critical role in the response of structures to various levels of strain. These properties are influenced by both the physical properties and loading characteristics of the soil material (Humar 2012, Dutta *et al.* 2017, Dash and Sitharam 2011, Shivaprakash and Dinesh 2018, DCF 1997, Malagnini 1996, Mulilis *et al.* 1978, Cevik and Cabalar 2009). Many studies have been conducted to investigate the impact of cyclic loading on the dynamic properties of soils, including fine-grained soils (Okur and Ansal 2007), sandy soils (Wang *et al.* 2011), organic soils (Geng *et al.* 2018), frozen silty soils (Wu *et al.* 2019), sand-gravel mixtures (Xu *et al.* 2019), and sand-silt mixtures (Meidani *et al.* 2008). The effects of particle size, angularity, and amount of granular materials have also been studied in relation to the cyclic behavior of soils (Shafiee *et al.* 2008, Soroush and Soltani-Jigheh 2009, Hassanipour *et al.* 2011). Additionally, loading frequency and waveform

have been shown to impact the dynamic properties of sandy materials (Araei *et al.* 2012). Other studies have investigated the impact of clay percentage on the psychometric and dynamic properties of soils (Kirar and Maheshwari 2013, Mominul 2013, Lei *et al.* 2016, Zhu *et al.* 2021, Aghaei Araei and Ghodrati 2018). Furthermore, the influence of different materials on the geotechnical properties of soils has been examined in studies on rubber content (Akbarimehr and Fakharian 2021), water pressure (Zhu *et al.* 2021) and the correlation between plasticity index and damping ratio (Darendeli 2001, Stokoe *et al.* 1995, Vucetic *et al.* 1998). Reviewing previous research, it is evident that several aspects of soil behavior have been studied, including the effect of loading frequency on the psychometric properties of sandy soil, the dynamic deformation and cyclic destruction of extremely soft soil, the mechanism of cohesive soil response, and the dynamic properties of mixed soils containing silt and sand. Furthermore, research has been conducted on mixed soils that contain fine-grained materials such as sandy soils, sands mixed with low to medium plasticity fine-grained materials, sands mixed with bentonite, and mixed sandy soils. Although most studies have focused on the dynamic behavior of pure sand or sand mixed with a concentrated layer, the dynamic properties of sand-silt mixtures have not been thoroughly examined. Moreover, there is a lack of research investigating the combined impact of loading frequency and the percentage of fine-grained silt on the dynamic properties of the shear modulus and Poisson's ratio of sand-silt mixtures. The stress-strain response of granular soils, specifically sand, at small, intermediate, and large

^{*}Corresponding author, Assistant Professor

E-mail: n.hadiani@gmail.com

^aPh.D. Student

E-mail: Alirezahasibitaheri@gmail.com

^bAssistant Professor

E-mail: ali.sadreddini@gmail.com

^cAssistant Professor

E-mail: zakeriiau@gmail.com

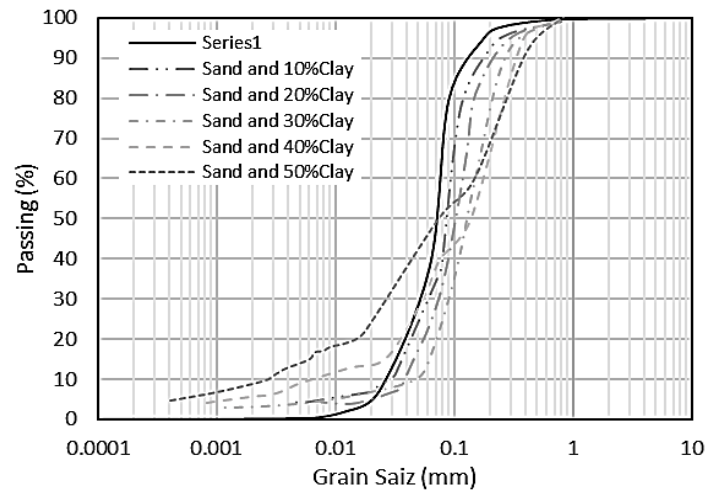


Fig. 1 Grain size distribution curve of 161 Firouzkouh sand materials and sand-silt samples

Table 1 Physical specifications of 161 Firouzkouh sand materials

D	D_{200}	D_{10}	D_{30}	D_{50}	D_{60}	C_U	C_e	e_{max}	e_{min}	G_s
amount	0.01	0.16	0.21	0.27	0.28	1.87	0.88	0.943	0.548	2.65

strains is influenced by various factors, including soil type, particle characteristics, particle size distribution, surface properties, and mineralogy. However, current research on the static and cyclic behavior of granular soils has primarily focused on clean and well-graded sands. This is problematic since in-situ soils often contain fines. The presence of a significant percentage of fines in silty sands can greatly impact their dynamic behavior, which requires careful examination. Moreover, earthquakes can produce highly complex excitations with a broad frequency range, and the frequency of an earthquake determines the shape of the waves transmitted through the soil. Soil layers have the ability to dampen vibrations at specific frequencies and amplify them at others. As such, the effect of fines content in silty sand mixtures on dynamic properties, especially in sand-fines mixtures, is an area of research that has not been thoroughly explored. It should be noted that a significant portion of earthquake energy is concentrated in the frequency range of 1 to 5 Hz (Li *et al.* 2022). However, previous studies have applied all cyclic deviatoric stresses uniformly in sinusoidal cycles at maximum frequencies of 0.2 Hz using triaxial tests, thereby overlooking the importance of loading frequency on dynamic behavior.

This study aims to investigate the impact of loading frequency, clay content and confining pressure on the dynamic properties of sand-clay mixtures using a cyclic triaxial apparatus under consolidated-undrained (CU) conditions. Sand-clay mixtures are commonly used in the construction of coastal structures and earth dams. In recent years, the need for a rational engineering approach for constructing structures on layers of sand-clay soil has increased, emphasizing the necessity for a proper understanding of the controlling factors that govern the behavior of these soils. Structures built on these soils are typically exposed to seismic loading or cyclic wave loads,

which may cause a decrease in stiffness, strength, and stability under undrained conditions. The performance of soil layers under excessively high loading conditions caused by earthquakes, winds, or waves is dependent on stress changes that occur under undrained conditions. Thus, studying the cyclic loading of sand-clay mixtures under undrained conditions is essential in providing valuable insights into the stress-strain behavior and resistance properties of these types of soils (Hight *et al.* 1991)

2. Material specifications and samples

The sand utilized in the samples was 161 Firouzkouh, which has a golden color and contains approximately 1% fine-grained particles. Table 1 provides a list of its physical properties, while Fig. 1 displays its grain size distribution curve and sand-silt composition grading. Additionally, the clay soil used in the samples belongs to the kaolin type.

The samples under investigation were 14 centimeters in height and 7 centimeters in diameter, prepared using the modified Proctor compaction method. Prior to creating each sample, three samples with different initial porosity ratios were subjected to the same compaction test, producing the same compaction line for each sample. Subsequently, the desired porosity ratio was estimated using this compaction line at the compaction pressure. The moisture distribution inside the sample by adding an equivalent moisture of 5% of the weight of each layer. The soil moisture was kept constant at this stage, and the percentage of moisture was prevented from changing. The sample was then poured into 7 layers inside the mold, and the surface was leveled. Using a hammer, each layer was compacted, and the height of each layer was controlled using the depth gauge. Table 2 outlines the specifications and number of three-axis cyclic

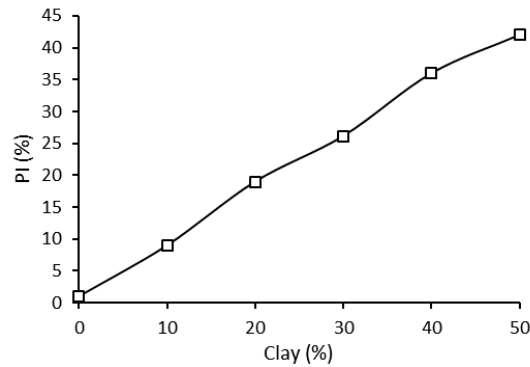


Fig. 2 Values of the shear modulus index for samples with different percentages of clay

Table 2 Characteristics of performed cyclic triaxial tests

Sample	Clay(%)	Loading Frequency (Hz)	σ' (kPa)	Number of tests
1	0	0.1, 1, 4	50, 100	6
2	10			6
3	20			6
4	30			6
5	40			6
6	50			6

tests performed. The addition of clay to the samples was based on a fixed volume ratio. The density for all samples was 1.656 g/cm^3 . As demonstrated in Fig. 2, an increase in the percentage of clay in each sample resulted in higher values of the plasticity index.

3. Methods

3.1 Cyclic triaxial test

Various methods and devices are available to conduct dynamic tests on soils. Among these, the cyclic triaxial device is a widely used device for testing different types of granular and cohesive geotechnical materials. The device comprises caps with porous stones that allow drainage of the sample required soil mass was determined by calculating the porosity ratio, specific gravity of particles, and volume. The total mass was divided by 7 to obtain the required mass for each layer. The water and soil were thoroughly mixed to achieve a uniform through the holes meant for water and CO_2 gas. In the cyclic triaxial test, the cell is first filled with water, and then the sample is subjected to multi-directional pressure by applying air pressure to the water inside the cell. The cell pressure and pore water pressure inside the sample are recorded separately. To apply the vertical force on the sample, a load cell and an actuator capable of generating dynamic loads are used on the rod, top cap, and finally, the sample itself. During the cyclic triaxial test, the change in sample volume is monitored by connecting the sample to the back pressure port, which also provides the necessary back pressure during the saturation of the sample. The cyclic triaxial test

device's components and details are shown in Fig. 3, including the load cell, actuator, top cap, porous stones, back pressure port, and water and CO_2 gas supply hoses.

3.2 Stages of conducting cyclic triaxial test

The Cyclic Triaxial test is conducted following the stages and loading procedures outlined in ASTM D3999 (2003). This test is performed under consolidated-undrained conditions, which ensures maximum similarity between soil loading conditions during earthquakes and cyclic triaxial testing. This is because drainage is not possible during high loading rates caused by earthquakes. In this study, the test is conducted under these conditions. The test stages include device preparation, sample preparation, sample construction, sample saturation, sample consolidation, and loading, which are explained below. Fig. 4 provides a schematic of the cyclic triaxial testing device.

The preparation stages of the triaxial device involve several steps, including placing the soil in an oven for 24 hours, preparing de-aired water, ensuring the absence of holes in the membrane, cleaning the porous stones, hoses, and connectors, and filling the back-pressure port with de-aired water.

The process of preparing a sample involves several steps. Firstly, a porous stone is placed on the bottom seat, and a smooth paper is placed on top of the stone. The membrane is then placed on the lower seat of the sample and sealed, followed by placing the lower seat mold and sealing it. The membrane is then wrapped around the mold, and a vacuum hose is connected to apply 20 kPa suction to attach the membrane to the mold. Soil is poured into 7 layers using the pounding method and leveled to create a

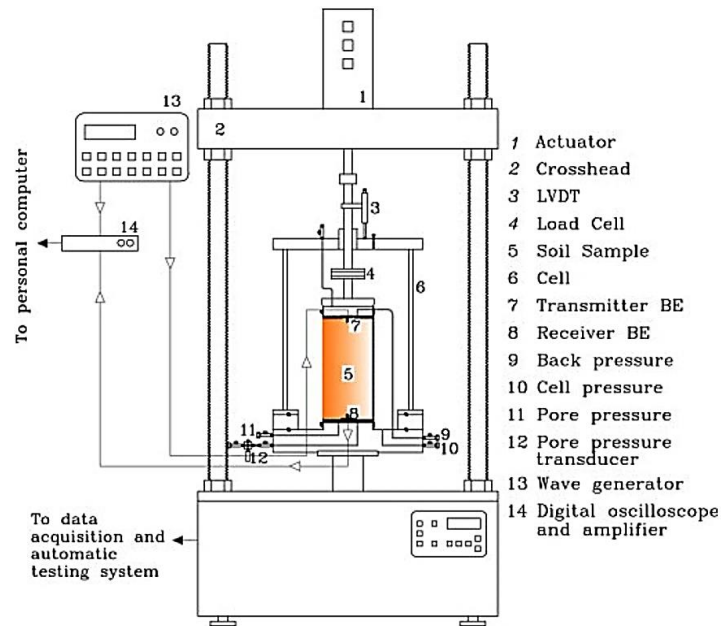


Fig. 3 Details and components of the cyclic triaxial testing device



Fig. 4 General view of the triaxial device

flat surface. A smooth paper is then placed on the sample, followed by placing a porous stone on the paper. Next, the upper part of the cell is transferred to the desired location, and the cap is placed on the porous stone. The fastening screws attached to the cap are tightened to prevent any unwanted volume change before consolidation. The upper part of the membrane is then sealed, and a hose is placed to connect the cap to the cell. Suction is transferred from the mold to the valve connected to the cap above the sample, and the mold is opened and removed from the cell. The bottom part of the cell is then cleaned, and plexiglass is placed on the o-ring. The o-ring is also cleaned, and the cell is filled with water. The bottom and top valves of the cell are closed, and the port hose is connected. The regulator is then adjusted to apply 20 kPa pressure to the water around the sample. Suction is removed from the sample, and the top and bottom valves of the sample are opened. If the sample is saturated, changes in pore water pressure during unconsolidated-undrained tests indicate a tendency for volume change in the sample, which is one of the valuable features of unconsolidated-undrained tests on saturated

samples. To saturate the sample, three steps are followed. CO₂ gas is passed through the sample, followed by passing air-free water, and finally taking the B-Value. CO₂ gas is heavier than air and has greater and faster solubility in water, which helps significantly in fully saturating the sample by replacing air particles with it. Air-free water is then passed through the sample, which dissolves most of the CO₂ in the cavities, and the remaining small amount is also dissolved in the water inside the sample. After saturation, the sample is consolidated. The effective stress of the sample increases in a drained process to consolidate the sample. Different types of consolidation stress paths can be tested by combining isotropic cell pressure and axial force.

3.3 Loading and calculation of parameters

The process of loading and parameter calculation can vary depending on the type of experiment. In this particular study, cyclic loading was applied without drainage, using biaxial stresses of 50 and 100 kPa and the cyclic stress range introduced by (Kramer 1996). The specimens were

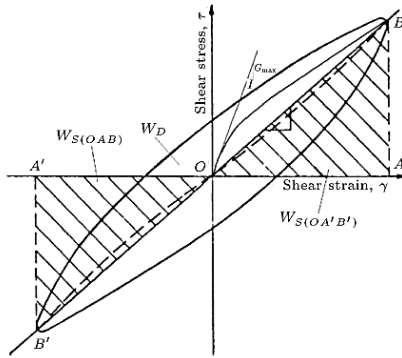


Fig. 5 Calculation of Shear Modulus and Damping Ratio Based on Hysteresis Curve (Aghaei Araei and Ghodrati 2018)

subjected to 40 loading cycles at three different frequencies: 0.1, 1, and 4 Hz. To obtain test results for the shear modulus and damping ratio as a function of shear strain, the first and last cycles were analysed based on the hysteresis loop shown in Fig. 5. Eqs. (1) and (2) were used to calculate the shear modulus and damping ratio. These equations use several parameters, including G (the shear modulus), D (the damping ratio), E (the elastic modulus), ν (the Poisson's ratio), W_D (the energy dissipated per cycle), and W_S (the maximum strain energy stored per cycle).

$$G = \frac{E}{2(1 + \nu)} \tag{1}$$

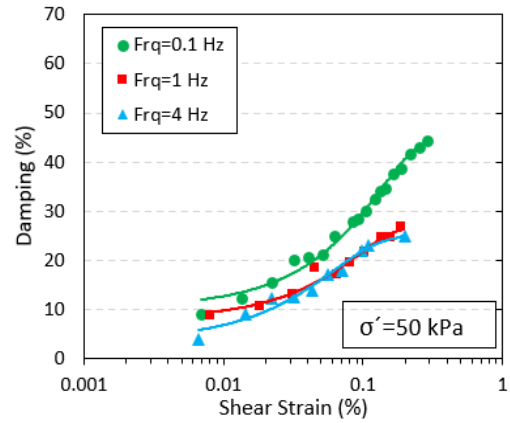
$$D = \frac{W_D}{2\pi(W_S(OAB) + W_S(OA'B'))} \times 100\% \tag{2}$$

4. Results

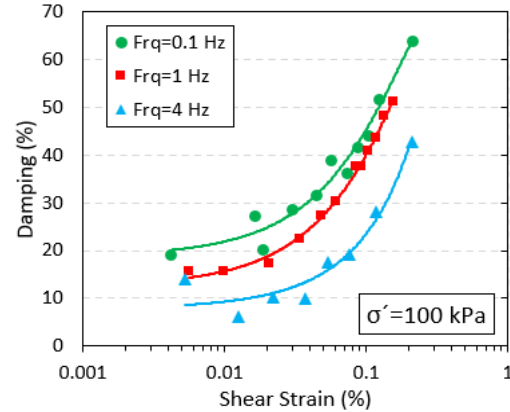
4.1 Effect of frequency and confined pressure

This section presents an analysis of 36 cyclic triaxial tests conducted on clean sand and sand-clay mixture. The variations of damping and shear modulus are examined under different frequencies of loading (0.1, 1, and 4 Hz) and confined pressures (50 and 100 kPa), as shown in Fig. 6. Results indicate that damping decreases as the frequency of loading increases, also as observed in Figs. 6(a) and 6(b), the effect of loading frequency on damping ratio changes are more considerable in $\sigma' = 100 \text{ kPa}$. The shear modulus of the clean sand sample is somewhat dependent on the frequency of loading, as illustrated in Figs. 6(c) and 6(d). Although the changes are not significant, an increase in the frequency of loading leads to an increase in the shear modulus.

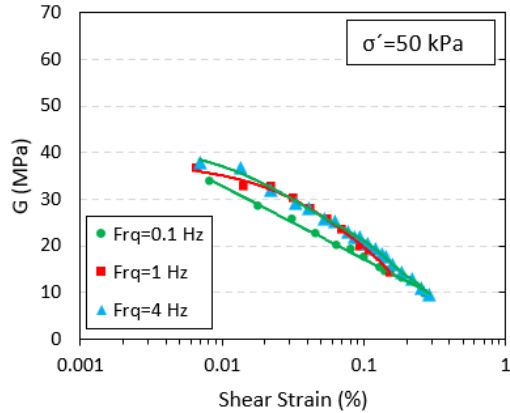
To facilitate a more comprehensive comparison of the impact of loading frequency and confining pressure on damping and shear modulus, comparative charts have been included in Figs. 7 and 8. As observed in Fig. 7, at $\text{Frq} = 0.1$, The alteration in damping ratio at a shear strain of 0.01% is nearly negligible, and gradually increases with a specific and constant trend with the increasing confining pressure at



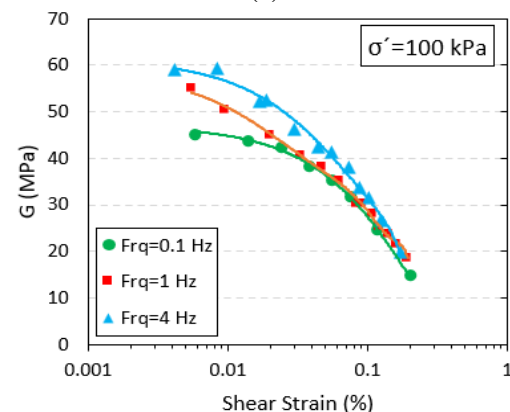
(a)



(b)



(c)



(d)

Fig. 6 Variations of Damping and Shear Modulus under Different Frequencies

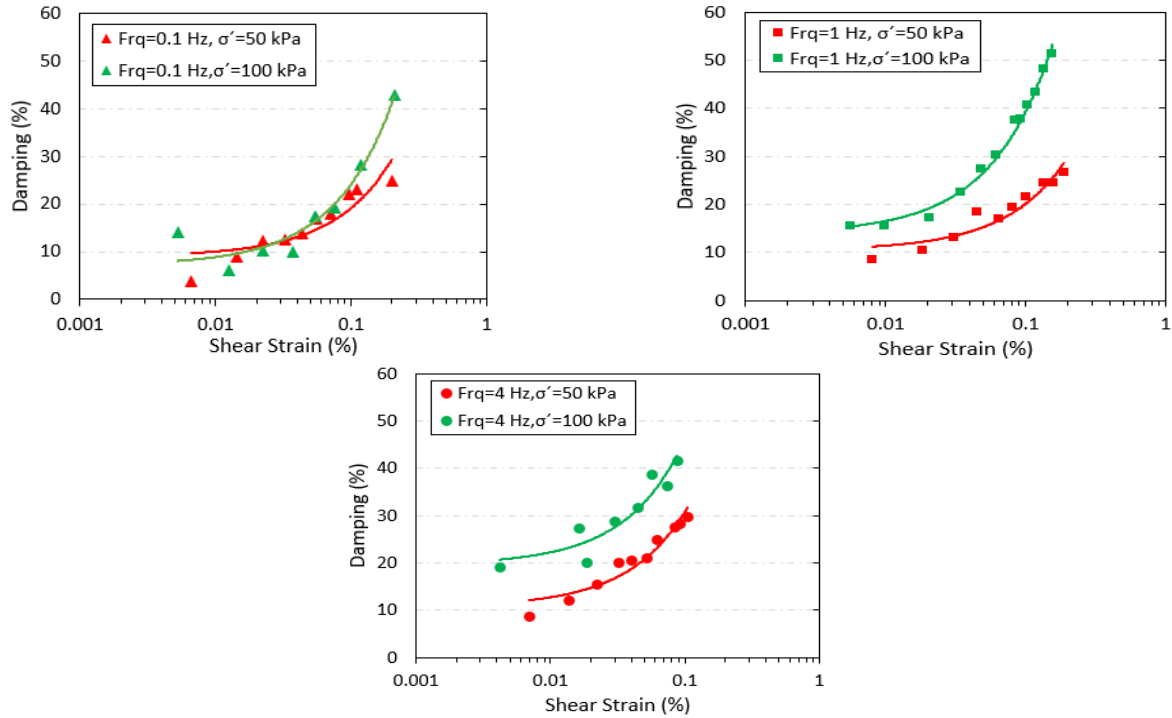


Fig. 7 Changes in Damping ratio at different frequencies and confining pressures

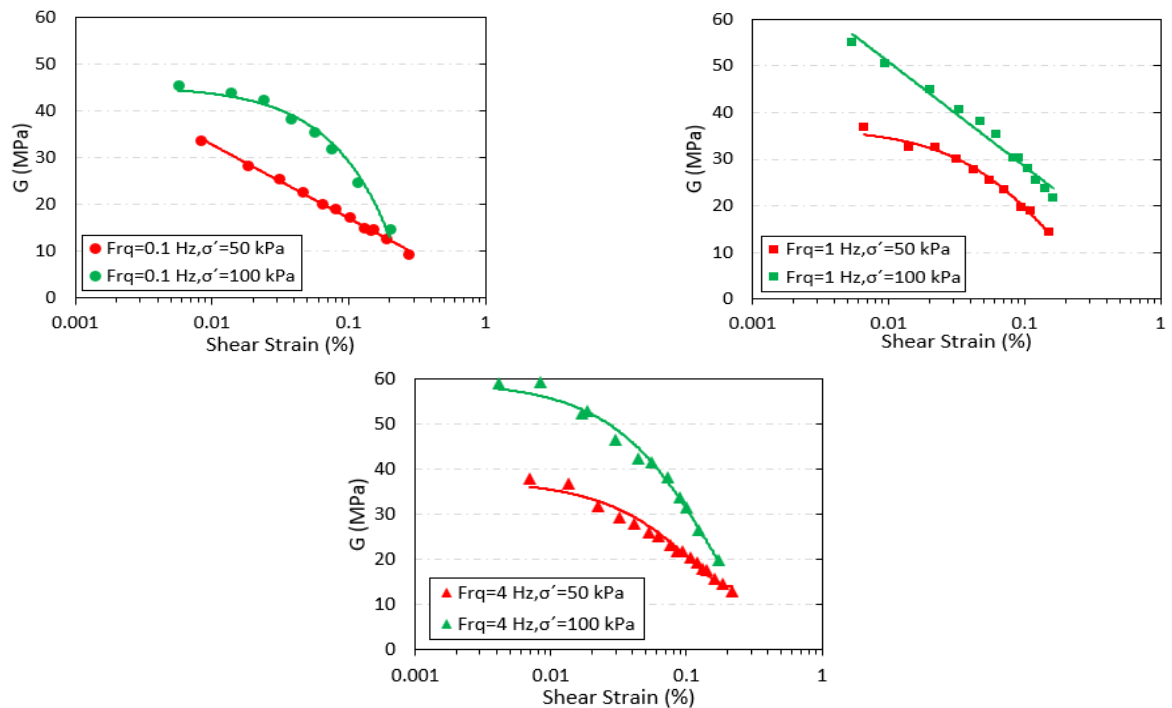


Fig. 8 Changes in shear modulus at different frequencies and confining pressures

higher shear strains. On the other hand, in Frq=1 and 4, the effects of confining pressure are remarkable even for low shear strain.

Fig. 8 display the changes in shear modulus at frequencies of 0.1, 1, and 4 Hz, respectively. These charts indicate that, the changes in loading frequency have an unremarkable effect on variation of shear modulus of clean sands.

4.2 Effect of increasing the percentage of clay content in samples

4.2.1 Damping ratio

In Fig. 9, the impact of clay content on damping is demonstrated. The findings reveal that the increase in clay content from 0 to 50% results in decreased damping for all sands.

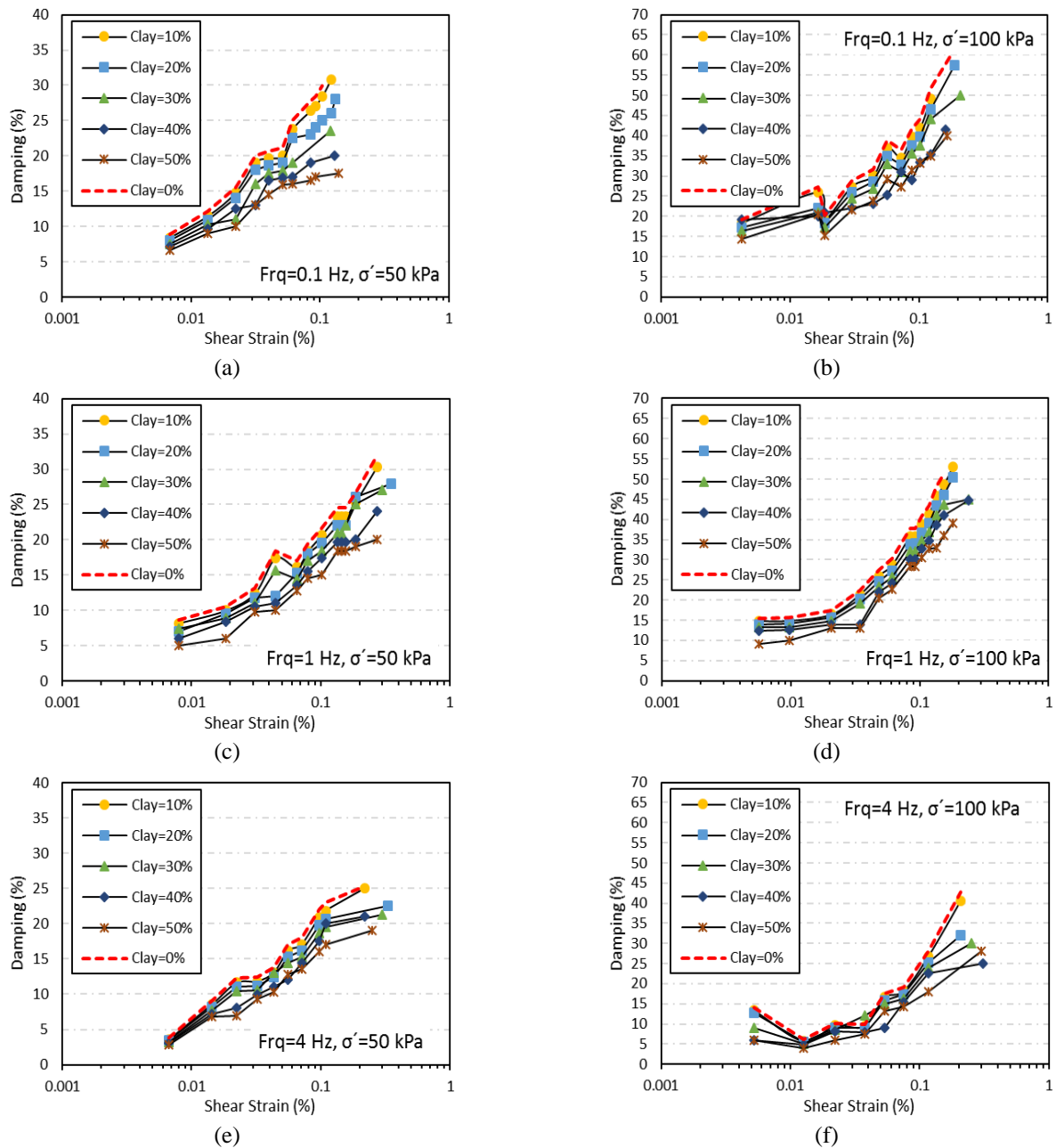


Fig. 9 Variation of Damping ratio with increasing percentage of clay in samples from 0 to 50%

three loading frequencies. Figs. 9(a), 9(c) and 9(e) demonstrate the damping changes for samples with varying clay content percentages under a lateral pressure of 50 kPa.

The results indicate a reduction in damping for samples with clay content percentages between 0 and 20%, with more pronounced effects observed for clay content percentages exceeding 30%. Figs. 9(b), 9(d) and 9(f) display the damping changes for samples under a confining pressure of 100 kPa. The results demonstrate minimal differences in damping reductions between confining pressures of 100 and 50 kPa.

As the sample becomes harder and the stress becomes more uniform, the damping ratio and energy dissipation ability decrease. This is due to a significant portion of the energy consumed in a sample or soil profile resulting from

the friction produced by soil particles sliding against each other. With an increase in uniform stress or any other parameter that causes soil to harden, the possibility of soil particle sliding and displacement on each other reduces, and, consequently, the damping ratio of the soil decreases.

4.2.2 Shear modulus

Fig. 10 explores the effect of varying percentages of clay on the shear modulus of samples at three different loading frequencies. The findings indicate that increasing the clay content from 0 to 50% results in a significant decrease in the shear modulus across all three loading frequencies. The magnitude of these changes for two different content pressure conditions is depicted in Figs. 10(a) to 10(f). While the trend of variations in the modulus of deformation

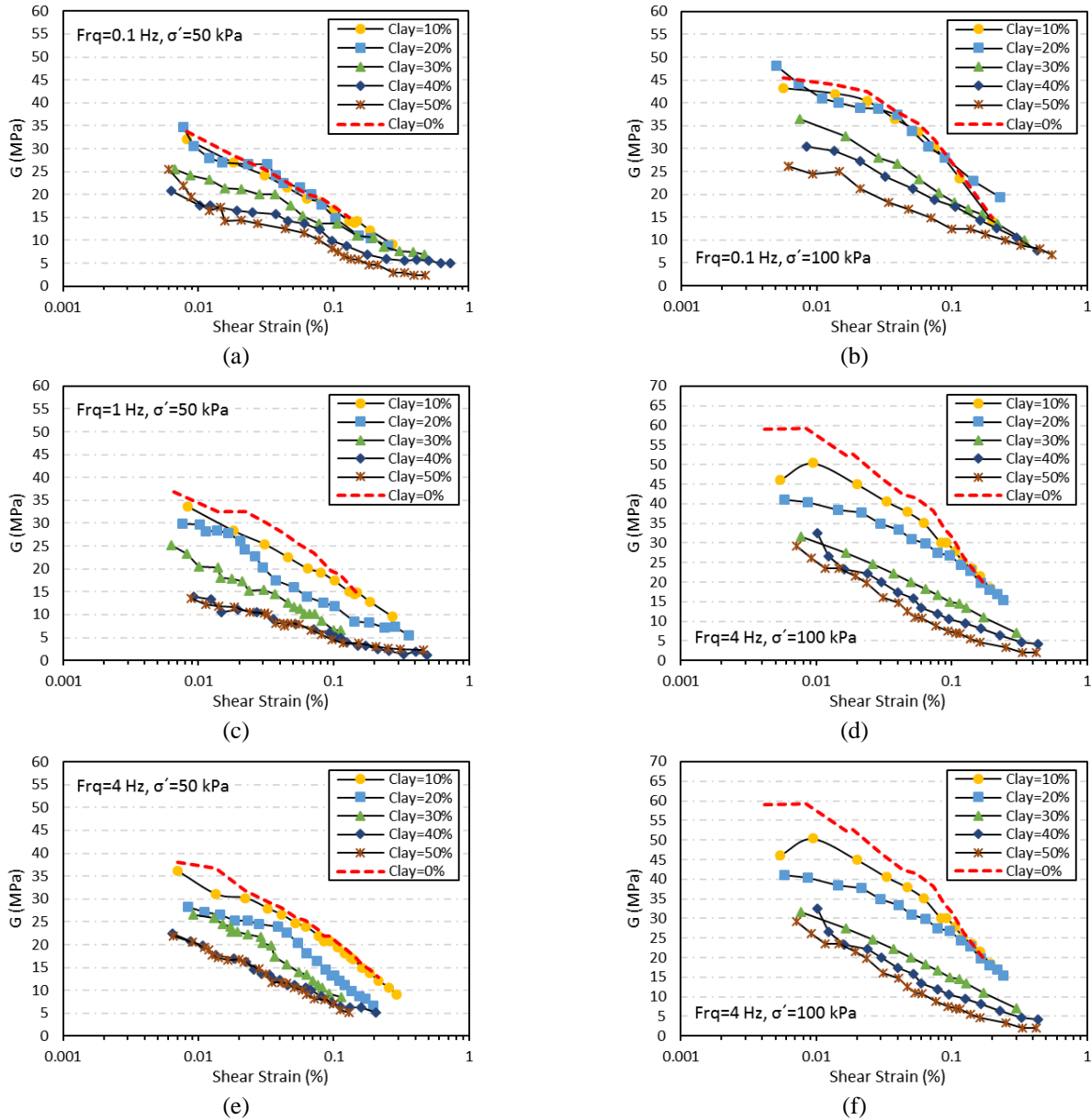


Fig. 10 Variation of shear modulus of samples with increasing percentage of clay from 0 to 50%

remains unaffected by confining pressure, altering the confining pressure from 50 kPa to 100 kPa leads to a change in the decreasing trend of the shear modulus of the samples. Comparing the pressure state diagrams of 50 kPa (Figs. 10(a), 10(c) and 10(e)) with those of 100 kPa (Figs. 10(b), 10(d) and 10(f)) shows that the effect of the clay content becomes more prominent with increasing lateral pressure. As the percentage of clay increases, a significant portion of the shear modulus decreases. Moreover, the results reveal that with an increase in the clay content from 30% to 40% and 50%, there is a sudden and severe decrease in the shear modulus compared to lower percentages of clay. This shift in trend is clearly evident in Figs. 10(b), 10(d) and 10(f). As confining pressure increases, the soil exhibits a wider range of linear behavior due to the hardening of the samples. With harder samples, soil grains can resist greater forces before sliding begins, leading to an increase in the range of linear behavior of the soil.

This paper utilizes the adapted Hardin-Drnevich model to characterize the G/G_{max} curve. To improve its accuracy in fitting, Darendeli introduced an extra parameter known as the curvature coefficient (n). The expression representing this model is as follows:

$$\frac{G}{G_{max}} = \frac{1}{1 + (\gamma/\gamma_r)^n} \quad (3)$$

where γ_r is the reference shear strain and it is the shear strain at $G/G_{max} = 0.5$ and n is the curvature coefficient.

In Figs. 11 and 12 variations in G/G_{max} are illustrated in correlation with changes in factors such as the content of clay, confining pressure, and loading frequency. It can be observed G/G_{max} can be reasonably captured by the empirical equation proposed by Seed and Idriss (1970). By comparing the graphs in both isotropic cases of 50 and 100, it becomes evident that the G/G_{max} increase with an

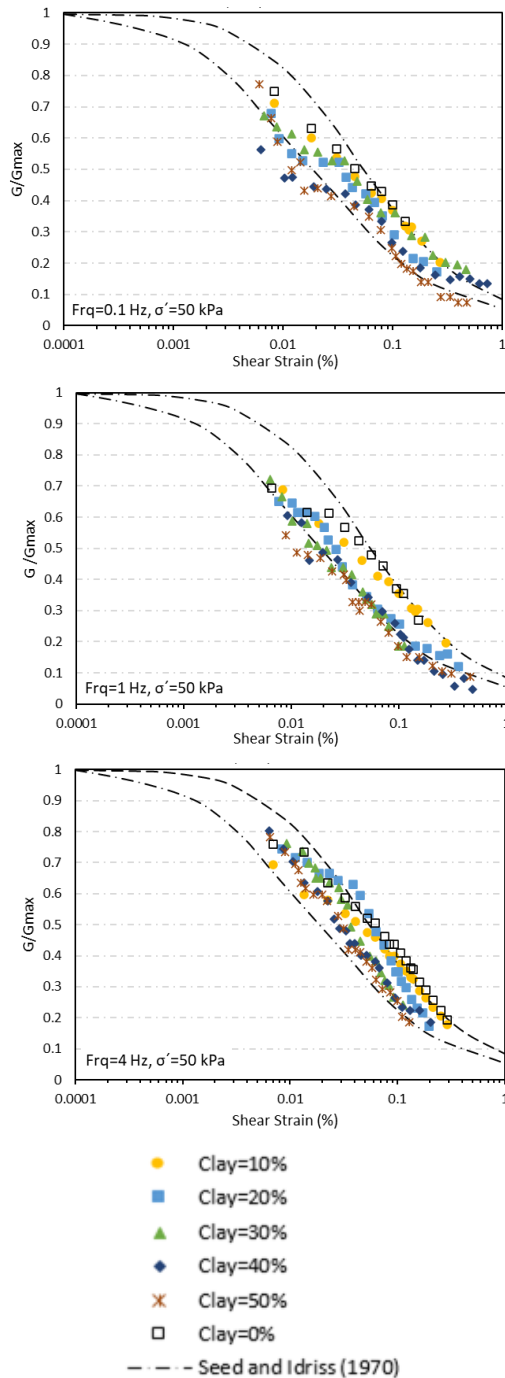


Fig. 11 Variation of shear modulus ratio of samples with increasing content of clay, $\sigma' = 50$ kPa

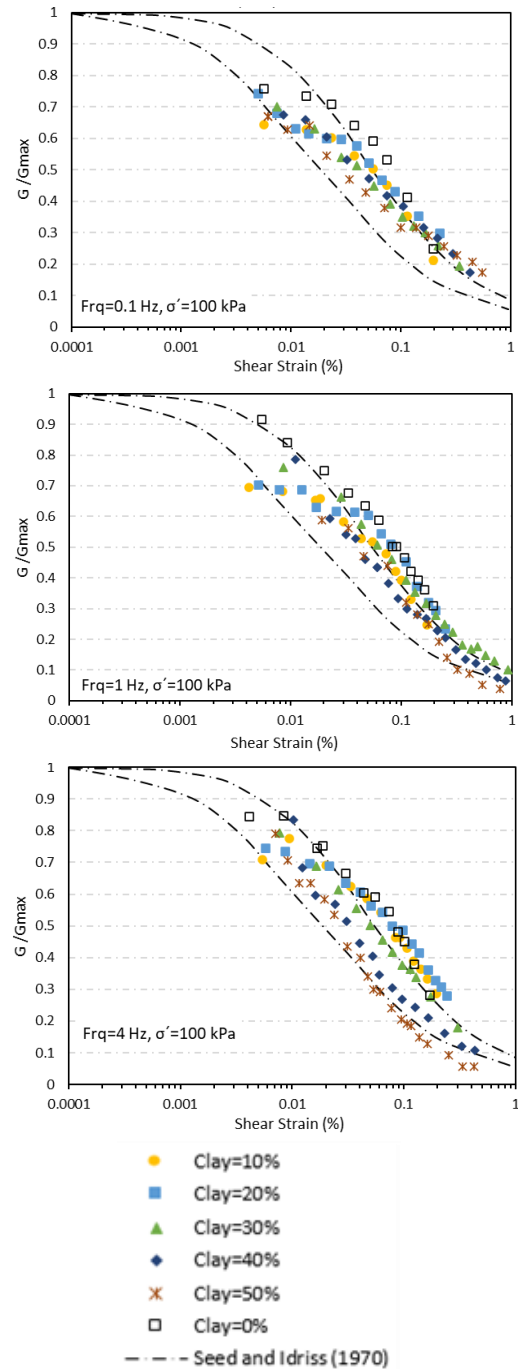


Fig. 12 Variation of shear modulus ratio of samples with increasing content of clay, $\sigma' = 100$ kPa

escalation in confining pressure. Furthermore, based on the presented graphs, as the content of clay increases, the G/G_{max} decrease. Specifically, as the clay content rises from zero to 50 percent, G/G_{max} experiences an approximate 20 percent reduction. This trend is nearly consistent across all frequencies, implying that the loading frequency will have a limited impact on G/G_{max} .

4.2.3 Hysteresis loops

The hysteresis loops of pure sand and sand-clay samples (30% clay) at different frequencies (0.1, 1, and 4 Hz) and confining pressure of 100 kPa and 20 cycles are presented

in Fig. 13. The loops display various differences attributable to a multitude of factors, including loading frequency. As the loading frequency rises, the hysteresis loop tends towards the vertical axis, and its slope with respect to the horizontal axis intensifies, indicating an increase in soil resistance (shear modulus) due to the frequency upsurge. Moreover, the hysteresis loops become elliptical as the frequency increases. Specifically, Figs. 13(b) and 13(c), depicting the hysteresis loop at a frequency of 4 Hz, display near-elliptical loops, signaling increased damping and energy dissipation. Various factors, including friction between soil particles, particle inertia, and viscosity of soil

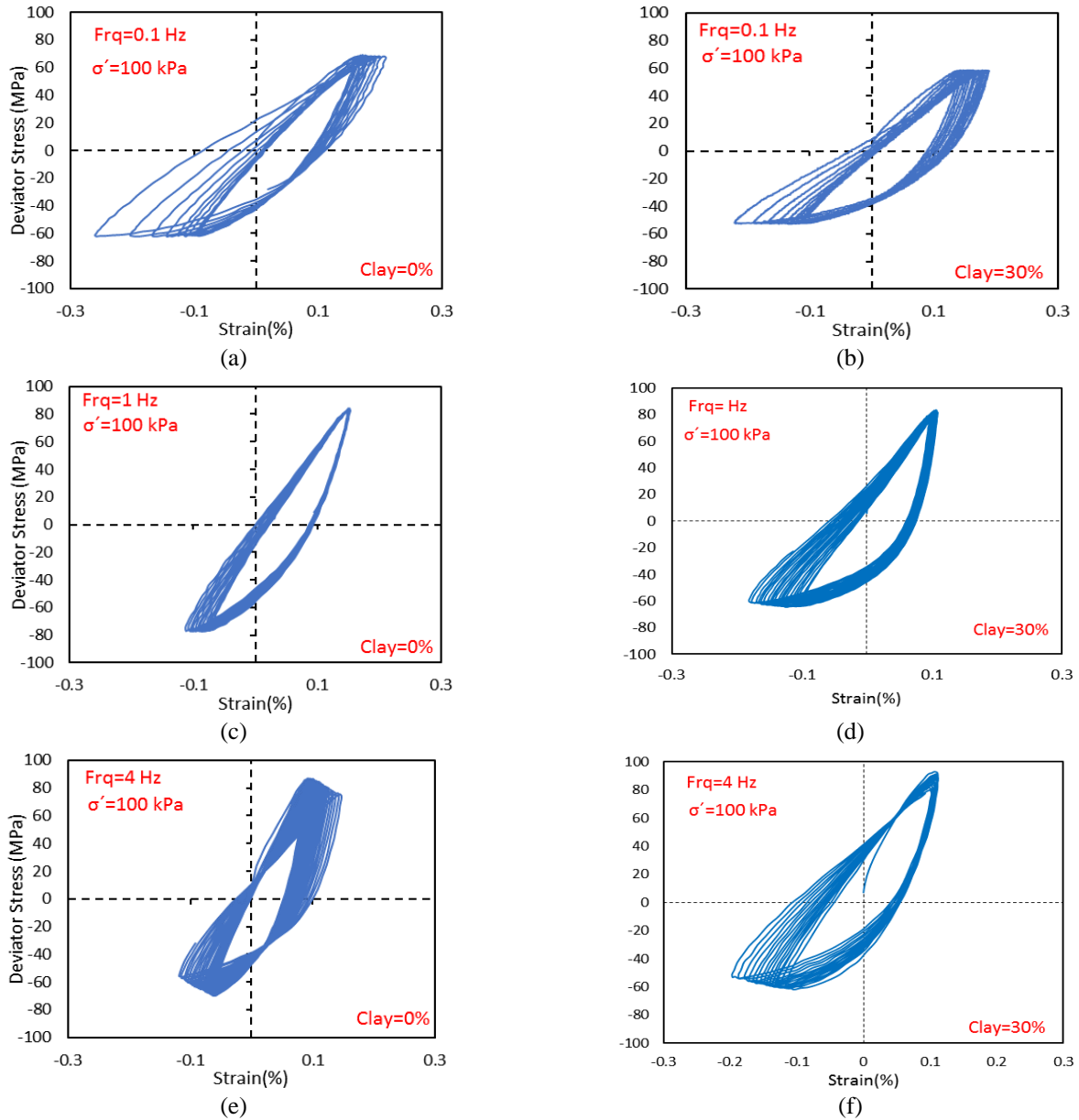


Fig. 13 Hysteresis loops of pure sand and sand-clay samples (30% clay) at different frequencies (0.1, 1, and 4 Hz) and confining pressure of 100 kPa

structure and pores, impact damping. Furthermore, the addition of 30% clay enhances damping and energy dissipation due to changes in particle inertia and soil structure viscosity.

To assess the impact of loading frequency on the hysteresis loops of samples, Figs. 14 and 15 depict the hysteresis loops for pure sand and sand-clay samples with 30% clay, respectively, at different frequencies (0.1, 1, and 4 Hz). As the loading frequency increases, the hysteresis loop approaches the vertical axis, signifying increased soil resistance (shear modulus) due to the frequency's escalation.

This behavior is consistent with the findings of Pandya and Sachan (2022), which investigated the impact of various loading frequencies (0.05, 0.1, 0.5, and 1 Hz) on soil hysteresis loops and reported that increasing the

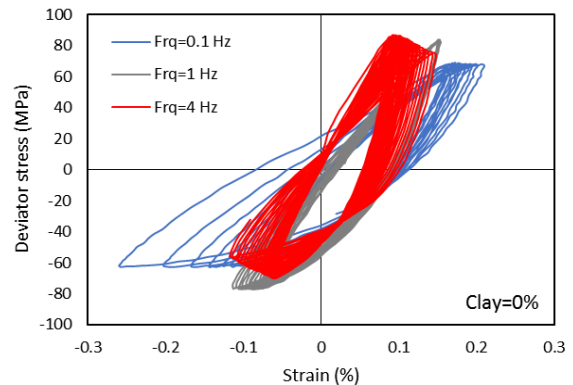


Fig. 14 Comparison of hysteresis loops of pure sand samples at different frequencies and confining pressure of 100

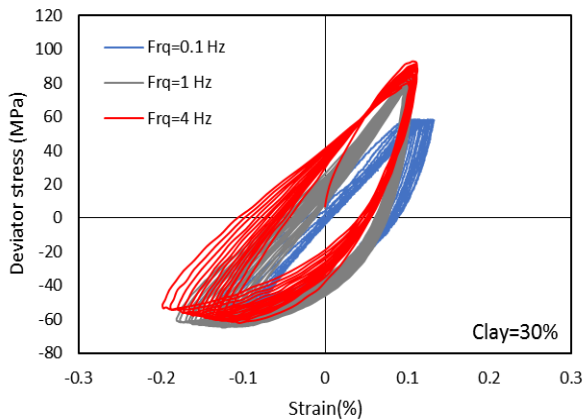


Fig. 15 Comparison of hysteresis loops of sand-clay samples (30% clay) at different frequencies and confining pressure of 100 kPa

frequency results in higher shear modulus and more elliptical hysteresis loops.

5. Conclusions

This study aimed to investigate the influence of loading frequency and clay content on the dynamic properties of sand-clay mixtures. A total of 36 cyclic triaxial tests were conducted to examine the effects of loading frequencies of 0.1, 1, and 4 Hz, clay content and confining pressures of 50 and 100 kPa and on the dynamic properties of pure sand and sand mixtures with 5% silt. The results revealed that the shear modulus of the soil increased with increasing confining pressure, while the energy dissipation and damping ratio decreased with increasing shear strength and confinement of the sample. Furthermore, the damping ratio of the sand sample decreased, and the shear modulus increased with an increase in loading frequency. Comparing the dynamic properties of pure sand and sand-silt mixtures showed that adding fines to the sand sample reduced the shear modulus and damping properties.

The study also found that:

- Increasing the fines content from 0 to 50% caused a significant decrease in the shear modulus of the samples at all three loading frequencies.
- Changing the lateral pressure from 50 kPa to 100 kPa resulted in a change in the decreasing trend of the shear modulus of the samples. The effect of fines content was more significant with increasing lateral pressure, and a significant portion of the shear modulus decreased with each step of increasing fines content.
- A sudden and severe decrease in the shear modulus was observed with fines content exceeding 30% (30%, 40%, and 50%). This indicates the effect of sample viscosity due to the addition of fines. However, it should be noted that the low effect of lower fines content on the consistency index resulted in a decrease in the shear modulus, and so on.
- Increasing the frequency of loading caused the hysteresis loop to rotate towards the vertical axis, indicating an

increase in the resistance of the samples (shear modulus) due to the increase in frequency. The hysteresis diagram tended to become more elliptical, indicating an increase in hysteresis loss and energy dissipation. Additionally, adding 30% clay content increased hysteresis and consequently energy loss in the samples.

Disclosure statement

The authors report there are no competing interests to declare.

References

- Aghaei Araei, A. and Ghodrati, A. (2018), "Loading frequency effect on dynamic properties of mixed sandy soils", *Sci. Iran*, **25**, 2461-2479. <https://doi.org/10.24200/sci.2017.4209>.
- Akbarimehr, D. and Fakharian, K. (2021), "Dynamic shear modulus and damping ratio of clay mixed with waste rubber using cyclic triaxial apparatus", *Soil Dyn. Earthq. Eng.*, **140**, 106435. <https://doi.org/10.1016/j.soildyn.2020.106435>.
- Araei, A.A., Razeghi, H.R., Tabatabaei, S.H. and Ghalandarzadeh, A. (2012), "Loading frequency effect on stiffness, damping and cyclic strength of modeled rockfill materials", *Soil Dyn. Earthq. Eng.*, **33**, 1-18. <https://doi.org/10.1016/j.soildyn.2011.05.009>.
- Cevik, A. and Cabalar, A.F. (2009), "Modelling damping ratio and shear modulus of sand-mica mixtures using genetic programming", *Exp. Syst. Appl.*, **36**, 7749-7757. <https://doi.org/10.1016/j.eswa.2008.09.010>.
- Darendeli, M.B. (2001), Development of a new family of normalized modulus reduction and material damping curves, The university of Texas at Austin.
- Dash, H.K. and Sitharam, T.G. (2011), "Undrained cyclic and monotonic strength of sand-silt mixtures", *Geotech. Geol. Eng.*, **29**, 555-570. <https://doi.org/10.1007/s10706-011-9403-3>.
- DCF, L.O.P. (1997), "Damping ratio of soils from laboratory and in situ tests," in "Seismic behaviour of ground and geotechnical structures", *Proceedings of the Special Technical Session on Earthquake Geotech. Engrg., 14th Int. Conf. on SMFE*, Balkema.
- Dutta, T.T., Saride, S. and Jallu, M. (2017), "Effect of saturation on dynamic properties of compacted clay in a resonant column test", *Geomech. Geoeng.*, **12**, 181-190. <https://doi.org/10.1080/17486025.2016.1208849>.
- Geng, M., Wang, D. and Li, P. (2018), "Undrained dynamic behavior of reinforced subgrade under long-term cyclic loading", *Adv. Mater. Sci. Eng.*, <https://doi.org/10.1155/2018/5685789>.
- Hassanipour, A., Shafiee, A. and Jafari, M.K. (2011), Low-amplitude dynamic properties for compacted sand-clay mixtures.
- Hight, D., Burland, J. and Georgiannou, V. (1991), Behaviour of clayey sands under undrained cyclic triaxial loading.
- Humar, J.: Dynamics of structures. CRC press (2012)
- Kirar, B. and Maheshwari, B.K. (2013), Effects of silt content on dynamic properties of Solani sand.
- Lei, H., Li, B., Lu, H. and Ren, Q. (2016), "Dynamic deformation behavior and cyclic degradation of ultrasoft soil under cyclic loading", *J. Mater. Civ. Eng.*, **28**, 4016135. [https://doi.org/10.1061/\(ASCE\)MT.1943-5533.0001641](https://doi.org/10.1061/(ASCE)MT.1943-5533.0001641).
- Li, X., Liu, J. and Nan, J. (2022), "Prediction of dynamic pore water pressure for calcareous sand mixed with fine-grained soil under cyclic loading", *Soil Dyn. Earthq. Eng.*, **157**, 107276. <https://doi.org/10.1016/j.soildyn.2022.107276>.
- Malagnini, L. (1996), "Velocity and attenuation structure of very

- shallow soils: evidence for a frequency-dependent Q”, *Bull. Seismol. Soc. Am.*, **86**, 1471-1486. <https://doi.org/10.1785/BSSA0860051471>. IC
- Meidani, M., Shafiei, A., Habibagahi, G., Jafari, M.K., Mohri, Y., Ghahramani, A. and Chang, C.S. (2008), Granule shape effect on the shear modulus and damping ratio of mixed gravel and clay.
- Mominul, H.M., Alam, M.J., Ansary, M.A. and Karim, M.E. (2013), “Dynamic properties and liquefaction potential of a sandy soil containing silt”, *Proceedings of the 18th international conference on soil mechanics and geotechnical engineering*, Paris.
- Mulilis, J.P., Townsend, F.C. and Horz, R.C. (1978), “Triaxial testing techniques and sand liquefaction”, *Dyn. Geotech. Test.*, **654**, 265.
- Okur, D.V. and Ansal, A. (2007), “Stiffness degradation of natural fine grained soils during cyclic loading”, *Soil Dyn. Earthq. Eng.*, **27**, 843-854. <https://doi.org/10.1016/j.soildyn.2007.01.005>.
- Pandya, S. and Sachan, A. (2022), “Effect of frequency and amplitude on dynamic behaviour, stiffness degradation and energy dissipation of saturated cohesive soil”, *Geomech. Geoeng.*, **17**, 30-44. <https://doi.org/10.1080/17486025.2019.1680885>.
- Seed, H.B. (1970), Soil moduli and damping factors for dynamic response analyses. Reoprt. EERC-70.
- Shafiee, A., Tavakoli, H.R. and Jafari, M.K. (2008), “Undrained behavior of compacted sand-clay mixtures under monotonic loading paths”, *J. Appl. Sci.*, **8**, 3108-3118. <https://doi.org/10.3923/jas.2008.3108.3118>.
- Shivaprakash, B.G. and Dinesh, S.V. (2018), “Effect of plastic fines on initial shear modulus of sand-clay mixtures”, *KSCE J. Civ. Eng.*, **22**, 73-82. <https://doi.org/10.1007/s12205-017-1076-x>.
- Soroush, A. and Soltani-Jigheh, H. (2009), “Pre-and post-cyclic behavior of mixed clayey soils”, *Can. Geotech. J.*, **46**, 115-128. <https://doi.org/10.1139/T08-109>.
- Standard, A. (2003), “Standard test methods for the determination of the modulus and damping properties of soils using the cyclic triaxial apparatus”, ASTM D3999/D3999M- 11 - 2013 - American Society for Testing.
- STOKOE II, K.H., Hwang, S.K., Lee, J.K. and Andrus, R.D. (1995), “Effects of various parameters on the stiffness and damping of soils at small to medium strains”, Pre-failure deformation of geomaterials, Proceedings of the international symposium, 12-14 September, 1994, Sapporo, Japan.
- Vucetic, M., Lanzo, G. and Doroudian, M. (1998), “Damping at small strains in cyclic simple shear test”, *J. Geotech. Geoenviron. Eng.*, **124**, 585-594. [https://doi.org/10.1061/\(ASCE\)1090-0241\(1998\)124:7\(585\)](https://doi.org/10.1061/(ASCE)1090-0241(1998)124:7(585)).
- Wang, Y., Wang, Y.L. and Zhang, S.M. (2011), “Study of effects of fines content on dynamic elastic modulus and damping ratio of saturated sand”, *Rock Soil Mech.*, **32**, 2623-2628.
- Wu, Z., Zhang, D., Zhao, T., Ma, J. and Zhao, D. (2019), “An experimental research on damping ratio and dynamic shear modulus ratio of frozen silty clay of the Qinghai-Tibet engineering corridor”, *Transp. Geotech.*, **21**, 100269. <https://doi.org/10.1016/j.trgeo.2019.100269>.
- Xu, D., Liu, H., Rui, R. and Gao, Y. (2019), “Cyclic and postcyclic simple shear behavior of binary sand-gravel mixtures with various gravel contents”, *Soil Dyn. Earthq. Eng.*, **123**, 230-241. <https://doi.org/10.1016/j.soildyn.2019.04.030>.
- Zhu, Z., Zhang, F., Peng, Q., Dupla, J.C., Canou, J., Cumunel, G. and Foerster, E. (2021), “Effect of the loading frequency on the sand liquefaction behaviour in cyclic triaxial tests”, *Soil Dyn. Earthq. Eng.*, **147**, 106779. <https://doi.org/10.1016/j.soildyn.2021.106779>.